Int. J. Engng Sci. Vol. 31, No. 3, pp. 435–451, 1993
Printed in Great Britain.

0020-7225/93 $6.00 + 0.00

DEPOSITION OF AEROSOLS ON SURFACES IN A TURBULENT CHANNEL FLOW

AMY LI and GOODARZ AHMADI
Department of Mechanical and Aeronautical Engineering, Clarkson University, Potsdam, NY 13699, U.S.A.

Abstract—A digital simulation procedure for studying deposition of aerosol particles in a turbulent channel flow is developed. An empirical mean velocity profile and the experimental data for turbulent intensities are used in the analysis. The instantaneous fluctuating velocities are simulated as continuous Gaussian random fields. Effects of Brownian diffusion, Saffman lift force, gravity and particle–surface interactions are included in the computational model. Starting with an initially uniform concentration near the wall, ensembles of particle trajectories are generated and statistically analyzed. Several simulations for deposition of aerosol particles of various sizes are performed and the corresponding deposition velocities are evaluated. The results are compared with the existing experimental data and those obtained by empirical equations. The effect of particle rebound from surface on particle deposition rate is also studied.

INTRODUCTION

Understanding the kinetics of aerosol dispersion has received considerable attention due to its significance in numerous industrial processes. The need of microelectronic industries to control microcontamination has motivated a number of new studies on the topic. Cooper [1] has provided a review of the needed microcontamination control research for microelectronic industries. Progress in analyzing particle deposition rate on wafers was reported by Cooper *et al.* [2] and Liu and Ahn [3]. In most practical applications, the air stream is turbulent and the particles are transported by the mean motion and are dispersed by turbulence fluctuations and Brownian diffusion. Fuchs [4], Davies [5], Friedlander and Johnstone [6], Cleaver and Yates [7] and Fichman *et al.* [8] provided semi-empirical expressions for particle mass flux from a turbulent stream to smooth surfaces. Particle deposition to rough walls was studied by Browne [9] and Wood [10]. Extensive reviews on the subject were provided by Wood [11], Hidy [12] and Papavergos and Hedley [13].

Computer simulation of aerosol dispersion has a long history. Ahmadi and Goldschmidt [14] used digital simulation and analytical techniques to study the turbulent dispersion of small spherical particles. Peskin [15] studied turbulent diffusion of particles in numerically simulated channel flow. Recently, Ounis and Ahmadi [16, 17] and Maxey [18] studied the dispersion of small particles in a numerically simulated random isotropic field. McLaughlin [19] and Ounis *et al.* [20, 21] computed the trajectories of rigid spherical particles in a channel flow using a pseudospectral computer code to simulate the instantaneous turbulent flow field. Rizk and Elghobashi [22] analyzed motions of particles suspended in a turbulent flow near a plane wall. Abuzeid *et al.* [23] and Li and Ahmadi [24] used a simple simulation technique to study the dispersion and deposition processes of suspended particles released from point sources in turbulent channel flows.

In this work, a digital simulation method for analyzing the deposition rate of aerosol particles on channel wall from a turbulent stream is described. The particle equation of motion includes the Brownian and Saffman lift forces in addition to the turbulent dispersion effect and gravity. An empirical mean velocity profile and the experimental data for turbulent intensities in the channel, are used for simulating the flow field. The instantaneous turbulent velocity field is modeled by a modified version of the Gaussian random field proposed by Kraichnan [25]. The Brownian motion is simulated as a white noise process. Starting with an initially uniform concentration near the wall, deposition velocities of particles in the range of 0.01–50 μm are

evaluated. Several coefficients of restitution, and and different materials for particle and surface are used and the effect of particle–surface interaction is studied. The results are compared with the available experimental data and those obtained from empirical equations.

PARTICLE EQUATION OF MOTION

The equation of motion of a small aerosol particle including the lift force is given by

$$\frac{du_i^p}{dt} = \frac{36\nu}{d^2(2S+1)C_c}(u_i - u_i^p) + \frac{2K\nu^{1/2}d_{ij}}{Sd(d_{lk}d_{kl})^{1/4}}(u_j - u_j^p) + \left(1 - \frac{1}{S}\right)g_i + n_i(t) \tag{1}$$

and

$$\frac{dx_i}{dt} = u_i^p, \tag{2}$$

where u_i^p is the velocity of the particle, x_i is its position, t is the time, d is the particle diameter, S is the ratio of particle density to fluid density, g_i is the acceleration of body force, $n_i(t)$ is a Brownian force per unit mass, ν is kinematic viscosity, $K = 2.594$ is the constant coefficient of Saffman's lift force, and u_i is the instantaneous fluid velocity with $u_i = \bar{u}_i = u_i'$, where $\bar{u}_i$ is the mean velocity of the fluid, and u_i' is the fluctuation component of fluid velocity. In equation (1), C_c is the Stokes–Cunningham slip correction given as

$$C_c = 1 + \frac{2\lambda}{d}(1.257 + 0.4e^{-1.1d/2\lambda}), \tag{3}$$

where λ is the molecular mean free path of the gas, and the deformation rate tensor d_{ij} is defined as

$$d_{ij} = \frac{1}{2}(u_{i,j} + u_{j,i}). \tag{4}$$

The lift force used in equation (1) is a generalization of the expression provided by Saffman [26] to a three-dimensional shear field.

SIMULATION OF TURBULENT FLOW FIELD

The mean velocity field in a channel as obtained in [27] is given by

$$\frac{\bar{u}}{\bar{u}_0} = \frac{1 - \eta^2 - \frac{k_v'}{k'}\frac{\cosh(k'\eta)}{\sinh k'} + \frac{k_v'}{k'}\frac{\cosh k'}{\sinh k'}}{1 + \frac{k_v'}{k'}\frac{\cosh k' - 1}{\sinh k'}}, \tag{5}$$

where $\eta = 1 - y/h$ is the nondimensional distance from the center line, h is the channel half width, k_v' and k' are nondimensional parameters defined as

$$k_v' = \frac{0.00703\,\mathrm{Re}^{0.763}}{1 - 0.71\,\mathrm{Re}^{0.0134}} - 2, \tag{6}$$

$$k' = k_v'\frac{1 - 0.71\,\mathrm{Re}^{0.0134}}{0.71\,\mathrm{Re}^{0.0134} - 0.5}, \tag{7}$$

Here, $\bar{u}_0$ is the mean centerline velocity and is given by

$$\bar{u}_0 = V/(0.71\,\mathrm{Re}^{0.134}), \tag{8}$$

where V is the mean channel velocity and

$$\mathrm{Re} = \frac{2\rho V h}{\mu}, \tag{9}$$

is the Reynolds number. In equation (9), ρ is the fluid mass density, and μ is the fluid viscosity. Good agreement between the predictions of equation (5) and the experiment data of Laufer [28] was reported in [27]. In this study, the mean velocity profile given by equation (5) is used.

Figure 1 shows the distributions of the turbulence intensities, $e_1(y) = \sqrt{u'^2}/u^*$, $e_2(y) = \sqrt{v'^2}/u^*$, $e_3(y) = \sqrt{w'^2}/u^*$, across the channel as given by Kreplin and Eckelmann [29]. These distributions are experimental data for a Reynolds number of 7700. In this figure, all intensities are nondimensionalized with respect to the shear velocity, $u^* = \sqrt{\tau_0/\rho}$, where τ_0 is the wall shear stress which is related to the friction factor f, i.e.

$$f = \frac{4\tau_0}{\frac{1}{2}\rho V^2} = \frac{8u^{*2}}{V^2}. \tag{10}$$

Here, an empirical equation [30] for the friction factor given by

$$\frac{1}{f^{1/2}} = -1.8 \log\left[\frac{6.9}{2\,\mathrm{Re}} + \left(\frac{\epsilon/h}{14.8}\right)^{1.11}\right], \tag{11}$$

is used. In equation (11), ϵ is the roughness of the wall and $\epsilon = 0$ for a smooth wall.

The turbulence fluctuations are random functions of space and time. The Monte-Carlo velocity simulation techniques have been used as an economical method for generating time histories that have the random character and statistical properties of turbulence. Kraichnan [25] suggested a simple method for generating a Gaussian random field which resembles a pseudo isotropic turbulence. Accordingly, the instantaneous fluctuating velocity is given as

$$\mathbf{u}'^*(\mathbf{x}^*, t) = \sqrt{\frac{2}{N}}\left\{\sum_{n=1}^{N} \mathbf{u}_1(\mathbf{k}_n)\cos(\mathbf{k}_n \cdot \mathbf{x}^* + \omega_n t^*) + \sum_{n=1}^{N} \mathbf{u}_2(\mathbf{k}_n)\sin(\mathbf{k}_n \cdot \mathbf{x}^* + \omega_n t^*)\right\} \tag{12}$$

In this equation,

$$\mathbf{u}_1(\mathbf{k}_n) = \zeta_n \times \mathbf{k}_n, \qquad \mathbf{u}_2(\mathbf{k}_n) = \xi_n \times \mathbf{k}_n, \tag{13}$$

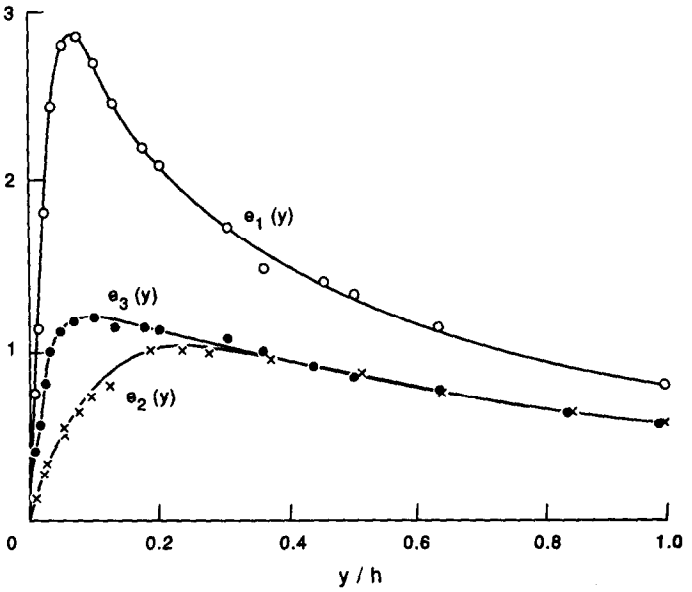

Fig. 1. Distributions of nondimensional turbulence intensities.

with

$$\mathbf{k}_n \cdot \mathbf{u}_1(\mathbf{k}_n) = \mathbf{k}_n \cdot \mathbf{u}_2(\mathbf{k}_n) = 0, \tag{14}$$

insures the incompressibility condition. The components of vectors ζ_n and ξ_n and the frequencies ω_n are picked independently from a Gaussian distribution with a standard deviation of unity. Each component of $\mathbf{k}_n$ is a Gaussian random number with a standard deviation of 1/2. Here, N is the number of terms in the series.

In equation (12), the dimensionless quantities are defined as

$$x^* = \frac{x}{l_0}, \qquad t^* = \frac{t}{t_0}, \qquad u_i'^* = \frac{u_i'}{u^*}, \tag{15}$$

where l_0, t_0 and u_i^* are local scales of turbulence and u' is the fluctuation fluid velocity which is assumed to be isotropic. For this pseudo turbulent velocity field the energy spectrum $E(k)$ is given as

$$E(k) = 16(2/\pi)^{1/2} k^4 e^{-2k^2}. \tag{16}$$

The experimentally measured root-mean-square (r.m.s.) fluctuation velocities shown in Fig. 1 are clearly nonisotropic. In this study, the fluctuation velocity given by equation (12) is modified in order to make it suitable for generating the nonisotropic instantaneous velocity field in the channel. It is assumed that

$$u_i' = u_i'' e_i(y), \quad \text{(no sum on } i\text{)} \tag{17}$$

where $e_i(y)$ are the shape functions for the axial, vertical and transverse r.m.s. velocities as given in Fig. 1.

The normal component of turbulence fluctuation near a wall has a profound effect on the deposition rate of particles. Therefore, the magnitude of $e_2(y)$ must be correctly evaluated for small values of y. It is well known [31] that v' has a quadratic variation at short distances from the wall, i.e.

$$v' \sim y^2 \quad \text{as} \quad y^+ \to 0. \tag{18}$$

In this study

$$e_2(y) = Ay^{+2} \quad \text{as} \quad y^+ < 2, \tag{19}$$

with $A = 0.0278$ is used, in order to match the data given in Fig. 1. Here

$$y^+ = yu^*/\nu, \tag{20}$$

is the distance from the wall, in wall units, and $\nu = \mu/\rho$ is the kinematic viscosity of fluid.

Estimates for the length and time scales of turbulence for wall bounded flows were provided in [32]. These are

$$l_0 = 0.1h(2\,\mathrm{Re})^{-1/8}, \tag{21}$$

and

$$t_0 = \frac{l_0}{u^*} = \frac{2h}{20u^*(2\,\mathrm{Re})^{1/8}} = \frac{h}{2V}. \tag{22}$$

Equations (12) and (17), with $N = 100$, together with (21) and (22), are used for simulating the fluctuation components of turbulent velocity in the channel.

It should be pointed out that the procedure used here for simulating the turbulent fluctuating velocity is quite different from that of Abuzeid *et al.* [23]. In [23], a Gaussian noise model was used which has a small correlation time of the order of Δt. The present smoothly varying Gaussian model has a more appropriate longer correlation time and its spectral behavior as

given by equation (16) is more representative of a real turbulent flow. The direct simulation of McLaughlin [19] and Ounis *et al.* [21], while being exact, is computationally too demanding for practical applications and it is also limited to low Reynolds number flows.

BROWNIAN MOTION

For submicron particles, the effect of Brownian motion becomes significant. To include such effects in the simulation, the Brownian force $n_i(t)$ is modeled as a Gaussian white noise random process [20, 23, 33–36] with spectral intensity S_{ij}^n given by

$$S_{ij}^n = S_0 \delta_{ij}, \tag{23}$$

where

$$S_0 = \frac{216 \nu k T}{\pi^2 \rho d^5 S^2 C_c}. \tag{24}$$

Here, T is the absolute temperature of fluid, $k = 1.38 \times 10^{-23}$ J/K is the Boltzmann constant. Amplitudes of the Brownian force components at every time step are then evaluated from

$$n_i(t) = G_i \sqrt{\frac{\pi S_0}{\Delta t}}, \tag{25}$$

where G_i are zero-mean, unit variance independent Gaussian random numbers and Δt is the time step used in the simulation.

An alternative procedure for simulation of Brownian motion was described by Gupta and Peters [35]. Their method is based on the solution of the corresponding Fokker–Planck equation for a small time step. In the present method, however, the Brownian force is directly simulated as a white noise process and is added to the equation of motion of the particle. As a result, it is somewhat simpler than the technique of [35] and it is more flexible in that the coupling effects with other forces could be easily accounted for.

PARTICLE–SURFACE INTERACTIONS

At low impact velocities, small particles that strike a surface adhere to it. However, as the impact velocity increases, the particle may rebound from the surface. Bounce occurs when the kinetic energy of a particle is sufficiently large to escape the attractive forces at the surface. The collision of a particle and a surface can be conveniently characterized in terms of the energy of particle–surface interaction and the critical approach velocity which is given by [24, 37–40]

$$V_c = \left[\frac{2E}{m}\left(\frac{1-r^2}{r^2}\right)\right]^{1/2}, \tag{26}$$

where r is the coefficient of restitution, E is the surface potential energy, and m is the mass of the particle. Capture or bouncing will occur when the particle normal approach velocity is less or greater than V_c.

According to Dahneke [38, 39], the surface potential energy is given by

$$E = \frac{Ad}{12 y_0}, \tag{27}$$

where A is the Hamaker constant, y_0 is the equilibrium separation of a particle and a surface (typically $y_0 = 4$ Å), and d is the diameter of the particle. The Hamaker constants for several materials were given by Dahneke [39]. For example, for gold–gold, silicon–gold, and quartz–gold particle–surface interactions, the corresponding Hamaker constants are 45.4×10^{-20}, 31.6×10^{-20} and 18.6×10^{-20}J, respectively.

RESULTS AND DISCUSSION

In this section, simulation results for deposition of particles from an initially uniform concentration of aerosols in a 2 cm wide channel are described. A temperature of 288 K, $\mu = 1.84 \times 10^{-5}$ N · s/m^2 and $\rho = 1.225$ kg/m^3 for air are used. A mean air velocity of $V = 5.0$ m/s in the channel is assumed. Thus, the flow Reynolds number based on the channel width is 6657 and the air is in a state of turbulent motion. Under these flow conditions, the friction velocity is about 0.3 m/s and one wall unit of length (ν/u^*) is about 50 μm. The corresponding wall unit of time (ν/u^{*2}) is 1.67×10^{-4} s. For this low Reynolds number flow, the half width of the channel is about 200 wall units. A density ratio of $S = 2000$ and different particle diameters ranging from 0.01 to 10 μm are used in these simulations. Silicon particles colliding with a gold surface with coefficient of restitution of 0.96, 0.85 and 0.5 are considered to study the effect of particle–surface interaction to deposition velocity. Ensembles of 3000 samples are employed for evaluating various particle trajectory statistics and wall deposition velocities. Table 1 shows a listing of the particle sizes used and the corresponding particle relaxation time $\tau = (Sd^2/18\nu)C_c$.

In present simulations the initial locations of particles are selected at random within 30 wall units so that the initial concentration is uniform in this region. The particle initial velocity is set equal to the local fluid velocity. To maintain the uniform concentration in the near wall region, a reflecting boundary condition is imposed at 30 wall units. When a particle leaves the 30 wall unit boundary, an identical particle is assumed to enter the region with opposite vertical velocity. Comparison of the present simulation results for deposition rate with the performed ones for the uniform concentration across the half width or the entire channel shows excellent agreement. That is almost all the deposited particles originate from an initial location with 30 wall units for the time duration of simulation (about 400 units of time or longer). Thus, limiting the simulation region to 30 wall units leads to considerable economy of needed computational time with no loss of accuracy.

The cases of vertical and horizontal channels are studied. In the former case, gravitation effect is neglected. For the horizontal flow channel, simulations are performed for the lower wall region for which the gravitational sedimentation would increase the particle deposition rate.

Vertical channel

Figure 2 shows the number of deposited particles versus the nondimensional time (t^+) for different particle diameters. Here,

$$t^+ = \frac{tu^{*2}}{\nu} \tag{28}$$

is the dimensionless time and ν/u^{*2} is the wall unit for time. As noted before, for a vertical channel, the effect of gravity is negligible. It is observed that the number of deposited particles increases rapidly at first and then reaches a quasi-equilibrium (roughly linear increase with

Table 1. Particle diameter and relaxation time

d (μm)	τ (s)	d^+	τ^+
0.01	2.00×10^{-8}	2.13×10^{-4}	1.37×10^{-4}
0.10	2.47×10^{-7}	2.13×10^{-3}	1.68×10^{-3}
0.50	2.60×10^{-6}	1.07×10^{-2}	1.78×10^{-2}
1.00	8.86×10^{-6}	2.13×10^{-2}	6.06×10^{-2}
2.00	3.26×10^{-5}	4.27×10^{-2}	0.222
3.00	7.10×10^{-5}	6.40×10^{-2}	0.485
5.00	1.92×10^{-4}	0.107	1.313
10.00	7.54×10^{-4}	0.2134	5.150

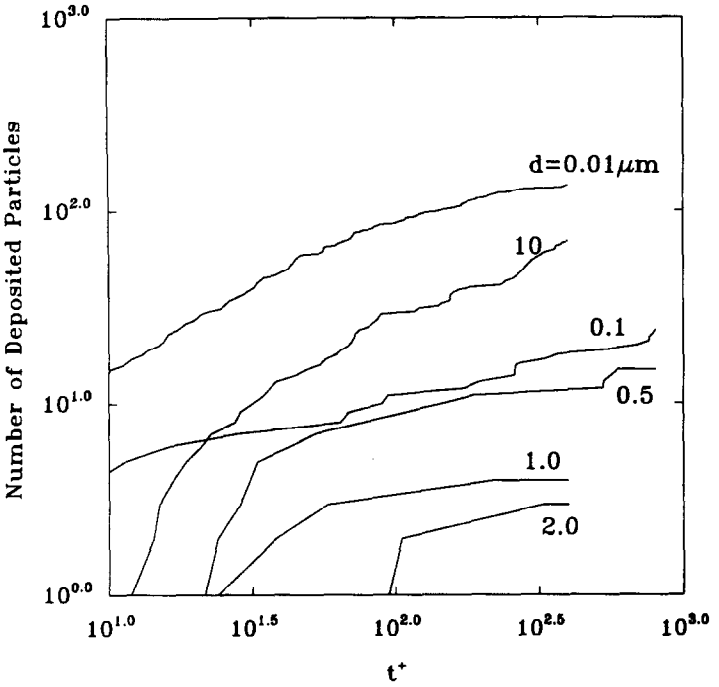

Fig. 2. Number of deposited particles vs time for a vertical channel.

time) condition. This figure shows that the number of deposited particles decreases as the particle diameter increases down to a minimum for sizes of about 2–5 μm (τ^+ of about 0.3–1.3) and then increases with further increase in diameter. For 0.01 μm particles (for which the Brownian diffusion is the dominant dispersion mechanism), about 130 particles deposit on the wall. For particles larger than 0.5 μm, the Brownian effect becomes negligibly small. For 3.0 and 5.0 μm diameters, only one particle deposits on the wall, which does not appear in Fig. 2. For 10 μm particles, the mechanism of turbulent eddy impaction becomes significant and about 80 particles deposit.

Figure 3 shows the sample time evolution of particle concentration within 30 wall units for different particles in the vertical flow channel. To evaluate the concentration, a bin of one wall unit is considered and the number of particles in each bin at a given time is evaluated. The initially uniform concentrations evolve as functions of time. At $t^+ = 400$, a general (turbophoresis) drift of particles toward the wall is observed from this figure. This is very similar to what was reported in [19, 43]. The number of particles within one wall unit also increases to about 200 particles. This is because the Brownian diffusion for 5 μm particles is practically negligible and, within the distance of one wall unit from the wall, the turbulent fluctuation is infinitesimal. The 5 μm particles that get there essentially just pile up, since there is no effective dispersion mechanism present.

For a uniform concentration of C_0 near a surface, the deposition velocity is defined as

$$u_d = J/C_0, \tag{29}$$

where J is the particle flux to the wall per unit time. The nondimensional deposition velocity given as

$$u_d^+ = u_d/u^*, \tag{30}$$

is commonly used in the literature as a convenient measure of particle flux to the wall. In simulation studies, when an initial number of particles N_0 is uniformly distributed in a region

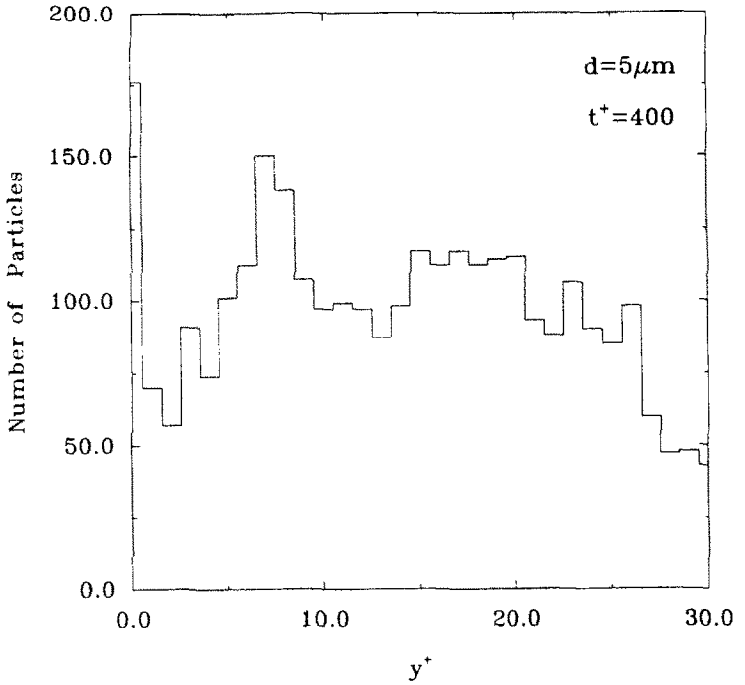

Fig. 3. Sample concentration of particles near the wall in a vertical channel.

within the distance of H_0^+ from the wall, the nondimensional deposition velocity is given by

$$u_d^+ = \frac{N_d/t_d^+}{N_0/H_0^+}, \tag{31}$$

where N_d is the number of deposited particles in the time duration t_d^+. In practice, t_d^+ should be selected in the quasi-equilibrium condition when N_d/t_d becomes a constant

Figure 4 shows variation of nondimensional deposition velocity with nondimensional particle relaxation time, defined as

$$\tau^+ = \frac{Sd^2u^{*2}}{18\nu^2} C_c. \tag{32}$$

In this figure, the hollow symbols are the present simulation results, and the dashed line is the result calculated from the empirical equation suggested by Wood [11] given as

$$u_d^+ = 0.057\,\mathrm{Sc}^{-2/3} + 4.5 \times 10^{-4}\tau^{+2}, \tag{33}$$

where Sc is the Schmidt number defined as

$$\mathrm{Sc} = \nu/D, \tag{34}$$

with D being the particle mass diffusivity. The experimental data as collected by Papavergos and Hedley [13], and simulation results given by McLaughlin [19] are also shown in this figure for comparison. It is observed that the simulation results are in agreement with the experimental data. The present result is also in qualitative agreement with the empirical equation given by (33) and the simulation of [19] in trend of variations.

Figure 5 shows the simulation results for the variation of deposition velocity with particle diameters. The prediction of equation (33) is also shown in this figure for comparison. It is observed that u_d^+ follows the expected V-shape curve variation. The minimum deposition velocity occurs for particle diameters in the range of 1.0–5.0 μm for the flow conditions used in this study. The simulation results are also in qualitative agreement with the empirical equation of Wood.

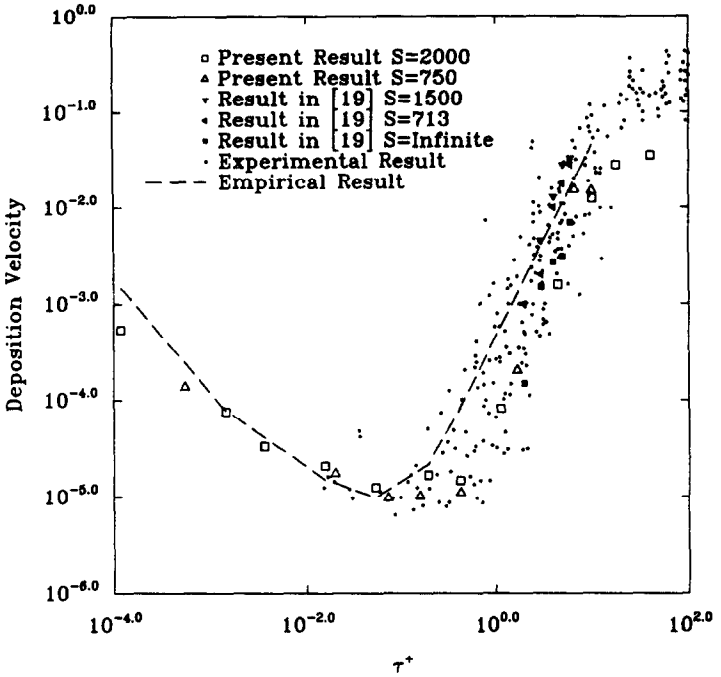

Fig. 4. Particle deposition velocity vs nondimensional particle relaxation time (τ^+) for a vertical channel.

Horizontal channel

Figure 6 shows the simulation results for the number of particles that deposit on the lower wall in a horizontal channel versus the nondimensional time (t^+) for different particle diameters. In this case, the effect of gravity is included in the equation of motion of the particle. Similar to the vertical channel case, the particle deposition rate is quite high at the beginning and approaches an equilibrium condition as time increases. It is observed that the

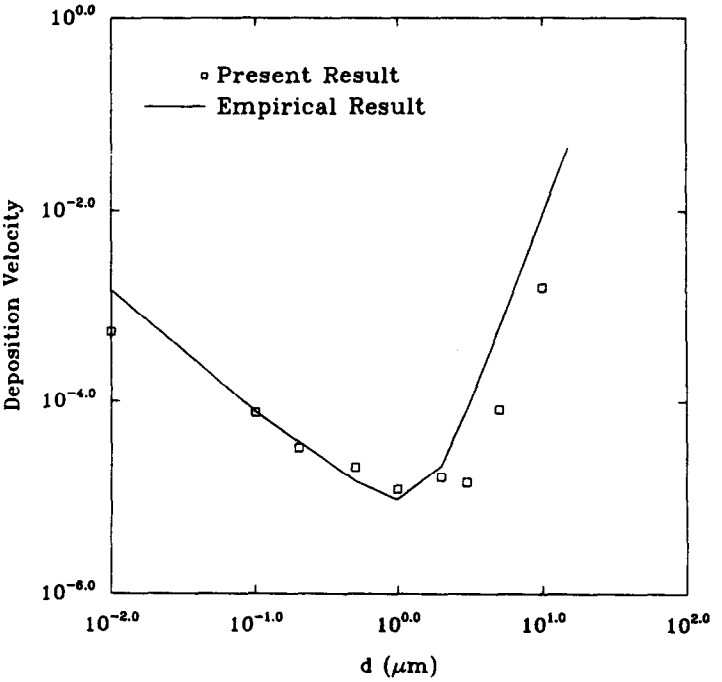

Fig. 5. Particle deposition velocity vs diameter for a vertical channel.

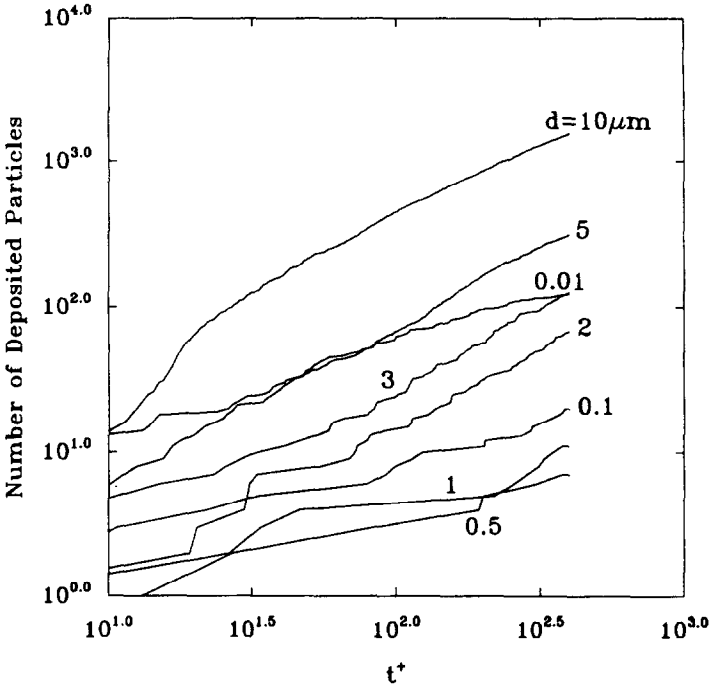

Fig. 6. Number of deposited particles vs time for a horizontal channel.

number of deposited particles is high for submicron particles and decreases as the particle diameter increases down to a minimum for particles of about 0.5 μm (τ^+ of about 1.8×10^{-2}) and then increases with further increase in diameter. Comparing Figs 2 and 6, it is observed that the gravitational sedimentation increases the deposition rate of particles larger than 1 μm, but has little effect on submicron particles. Figure 6 shows that 130 0.01 μm particles deposit on the wall which is identical to that for the vertical channel flow case. The gravity, however, significantly increases the number of deposited 5 and 10 μm particles to more than 200 and 1000, respectively.

Sample time evoluations of particle concentration within 30 wall units for the horizontal flow channel are shown in Figure 7. This figure shows that the drift of particles toward the wall is accelerated due to gravity and there is no particle pile up within one wall unit like the one observed in Fig. 3. The particles that reach the one wall unit region, now quickly sediment to the wall due to gravity.

In order to verify the accuracy of using only the 30 wall units region in our computer simulations, several simulations for uniform concentration of particles across the half width of the channel are also performed. Twenty thousand particles are uniformly distributed across the channel. This corresponds roughly to the concentration of 3000 particles in 30 wall units. The corresponding deposition rate is compared with the earlier simulation for the 30 wall units region in Fig. 8. It is observed that the results are in very good agreement. This implies that the simulations for 30 wall units are sufficiently accurate.

Figure 9 shows the variation of nondimensional deposition velocity with particle nondimensional relaxation time in horizontal channel which includes gravitational sedimentation. In this figure the solid line is the present simulation results, and the solid line corresponds to the prediction of the empirical equation given by Wood which is modified for gravitational effect, i.e.

$$u_d^+ = 0.057\,\mathrm{Sc}^{-2/3} + 4.5 \times 10^{-4}\tau^{+2} + \tau^+ g^+, \tag{35}$$

where the nondimensional acceleration of gravity is defined as

$$g^+ = \nu g / u^{*3}. \tag{36}$$

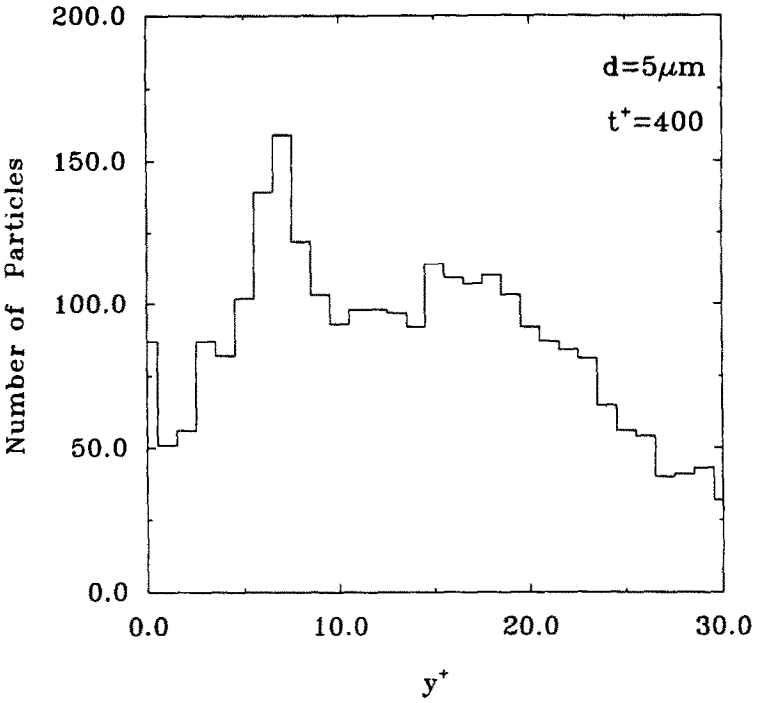

Fig. 7. Sample concentration of particles near the wall in a horizontal channel.

In equation (35), it is assumed that the gravitational effect is linearly additive to the Brownian and turbulent eddy impaction effects. A good agreement is observed between the present simulations and the empirical equation given by (35) when $\tau^+ > 0.05$.

Figure 10 shows the variation of deposition velocity with particle diameters for the horizontal channel including gravitational effect. The expected V-shape variation is clearly observed from this figure. Particle diameter for the minimum deposition rate is now 0.1–0.5 μm. This is an order of magnitude higher than that for the vertical channel shown in Fig. 5.

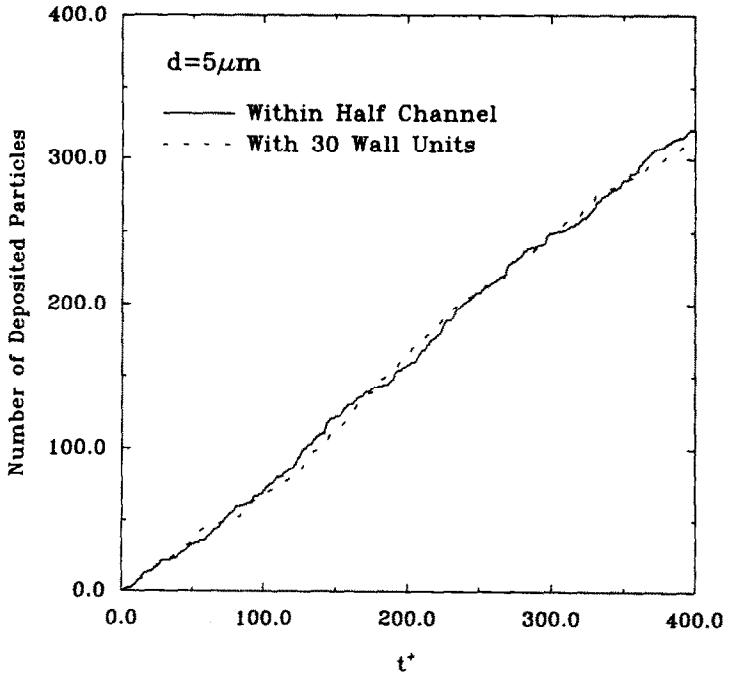

Fig. 8. Comparison of simulation results for within half channel with those for within 30 wall units.

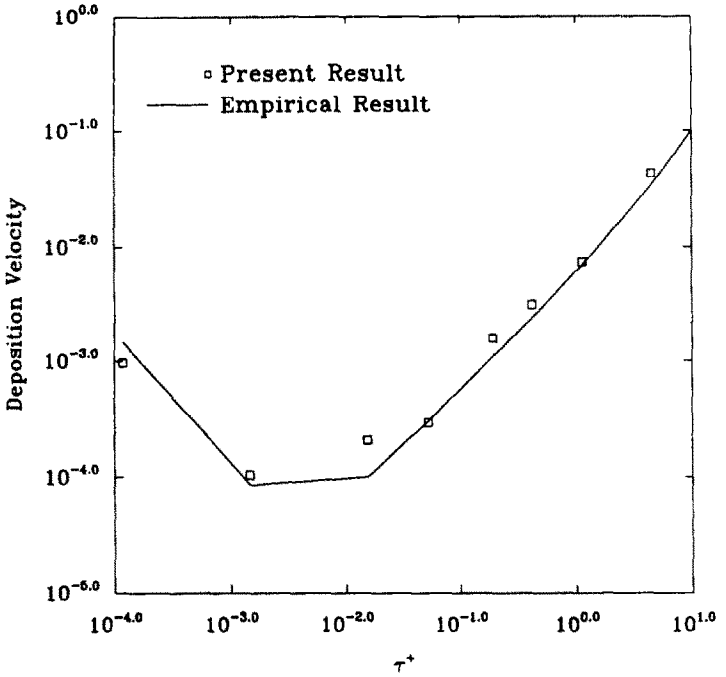

Fig. 9. Particle deposition velocity vs nondimensional particle relaxation time (τ^+) for a horizontal channel.

Particle–surface interaction effect

Sample particle trajectories including rebound effects in a vertical channel are shown in Fig. 11. It is assumed that the surface is coated with gold and the particles are nearly elastic ($r = 0.96$) and made of silicon. It is observed that the 20 μm particle, which is released from a point 30 wall units above the surface, rebounds four times before depositing on the wall. The 30 μm particle rebounds five times and is still suspended in the air stream after 400 wall units of time.

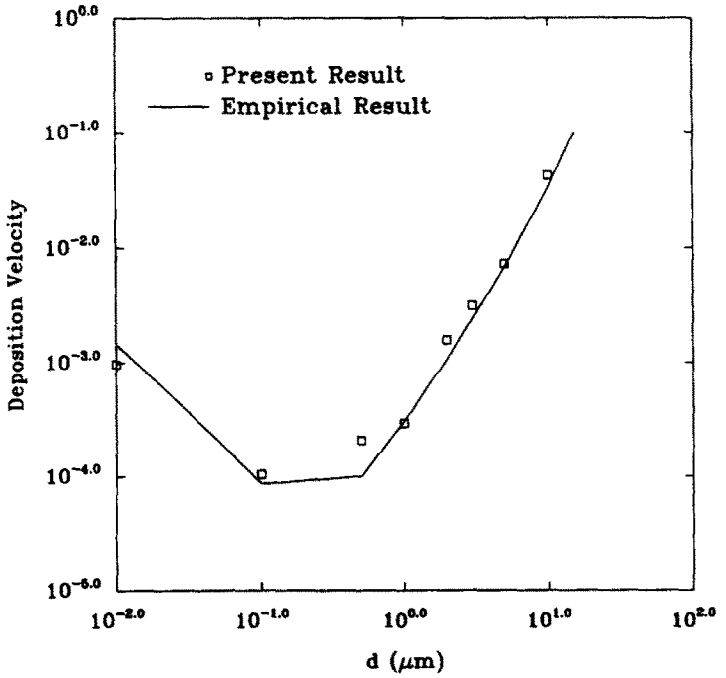

Fig. 10. Particle deposition velocity vs diameter for a horizontal channel.

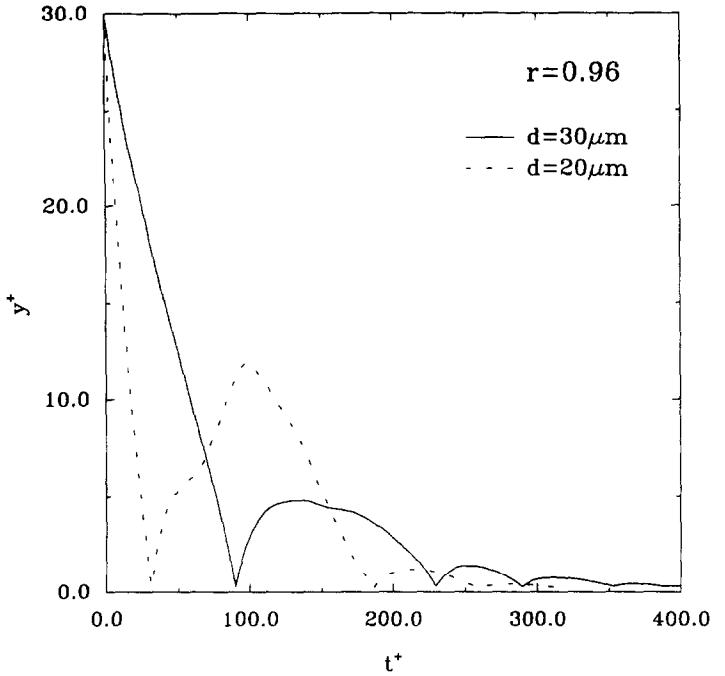

Fig. 11. Sample particle trajectories including rebound effect for a vertical channel.

Variation of the nondimensional deposition velocity with surface potential energy for 10 μm particles is shown in Fig. 12. Three different materials for particles are considered, while the surface is assumed to be gold. A coefficient of restitution of 0.96 is used. It is observed that the deposition velocity increases as surface potential energy increases. The gold–gold pair has a higher surface potential energy than those of silicon–gold and quartz–gold pairs. Thus, gold particles need higher kinetic energy to escape the attractive force of a gold surface. In the present simulation, for an ensemble of 3000 particles, about 60 gold particles deposit on the wall, while only about 50 silicon particles and 45 quartz particles are deposited on the surface.

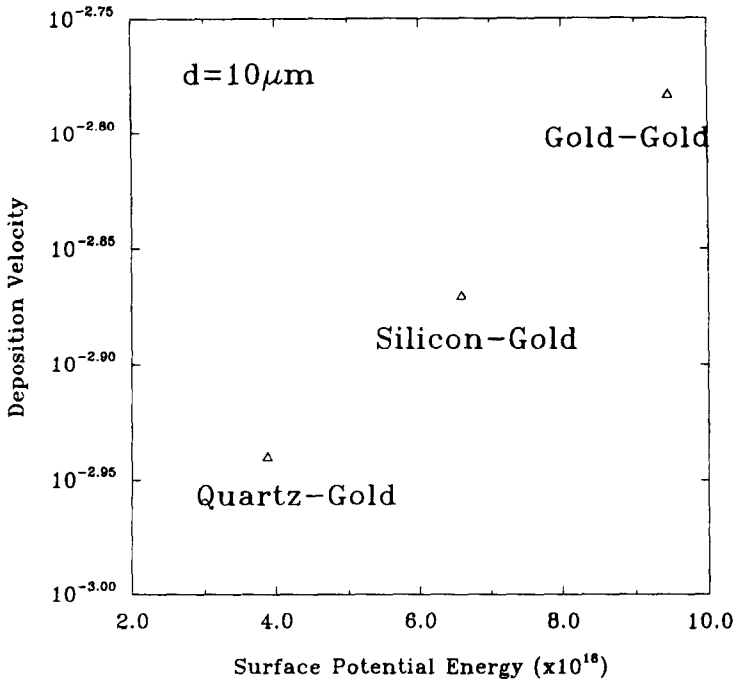

Fig. 12. Particle deposition velocity vs surface potential energy.

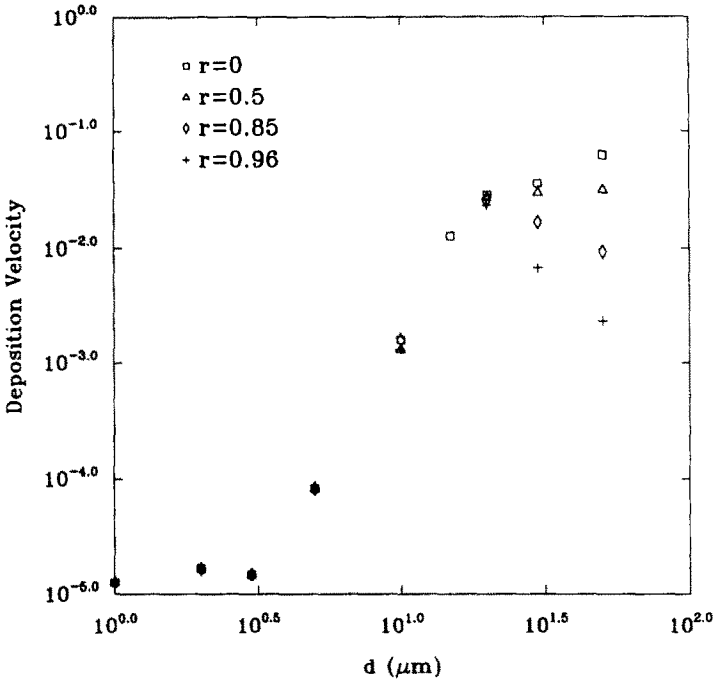

Fig. 13. Particle deposition velocity vs particle diameter including rebound effect for a vertical channel.

Figures 13 and 14, respectively, show variations of the nondimensional deposition velocity of silicon particles with diameter and particle relaxation time in the vertical channel with gold surfaces including the rebound effects. Several coefficients of restitution including $r = 0$ (no rebound) are considered for comparison. It is observed that particle rebound from the wall considerably reduces the deposition velocity for particles larger than $10\,\mu$m or for particle relaxation time large than 5. Effects of particle bounce are particularly noticeable for large

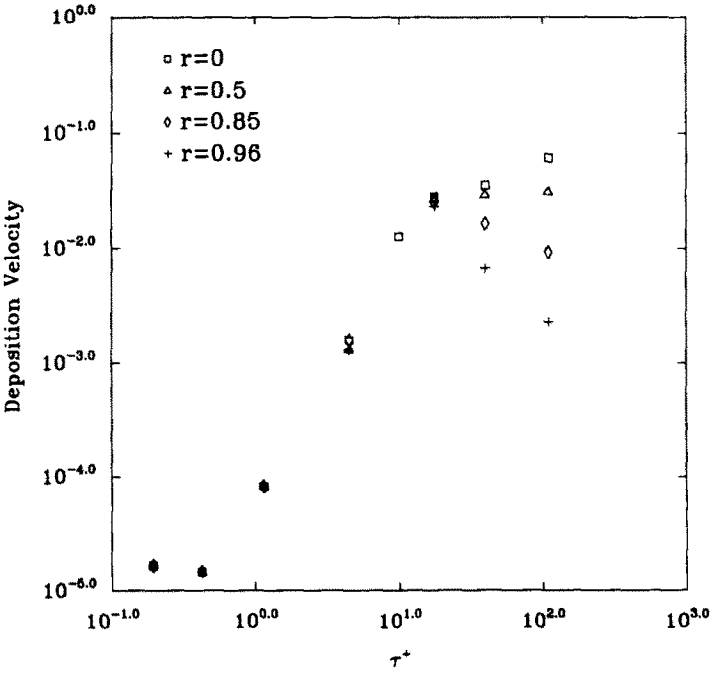

Fig. 14. Particle deposition velocity vs nondimensional particle relaxation time including rebound effect for a vertical channel.

coefficients of restitution. Furthermore, for $r > 0.85$ and $d > 30\,\mu m$ ($\tau^+ > 20$), the deposition-velocity decreases as the particle diameter or relaxation time increases. In this case, the peak deposition velocity occurs at a diameter of about $20\,\mu m$ (relaxation time of about 15).

The simulation results show that the effect of rebound for particles smaller than $5\,\mu m$ is negligible. This is because for particles smaller than $5\,\mu m$ (relaxation time less than 1), the critical approach velocity is rather large (larger than 1.1 cm/s). The surface impact velocities of these particles due to turbulence eddies are generally lower than the critical approach velocity. Thus, when these particles strike the wall, they adhere to it and almost no rebound occurs. For particles greater than $10\,\mu m$ (particle relaxation time greater than 5), the critical approach velocity is relatively small (smaller than 0.8 cm/s). In addition, these particles maintain their velocities, which are imparted to them by turbulent eddies, for a long duration of time. Therefore, when these large nearly elastic particles strike a surface at relatively high speed, they can easily escape the attractive forces and bounce from the surface. The probability of rebound increases as the size of the particle or the coefficient of restitution increases. For particles with $d \geq 20\,\mu m$, the simulation results show that most deposited particles bounce more than once before sticking to the wall. Some particles keep on bouncing and never deposit on the wall within the time duration used in the simulation.

Variations of nondimensional deposition velocity of silicon particles with diameter and particle relaxation time in the horizontal channel with gold walls including the rebound effects are displayed in Figs 15 and 16. The simulation results shown in these figures are the average deposition velocities during 100–400 wall units of time. The available experimental data from [13, 41] and the model predictions [11, 42] are also shown in these figures for comparisons. It is observed that the present simulation results are in reasonable agreement with the experiment data and theoretical models. Figures 15 and 16 show that the particle rebound effect considerably reduces the deposition velocity of particles with diameters larger than $10\,\mu m$ and/or relaxation times larger than about 5. The reduction of u_d^+ is particularly noticeable for particle diameter larger than $30\,\mu m$ ($\tau^+ > 40$) and coefficient of resititution larger than 0.85. The present simulation result has a trend of variation similar to the sublayer model of [42].

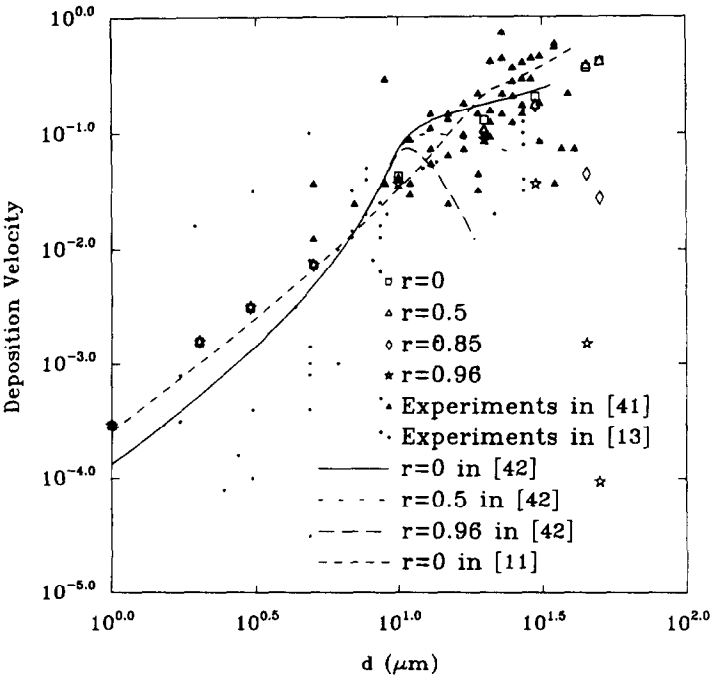

Fig. 15. Particle deposition velocity vs particle diameter including rebound effect for a horizontal channel.

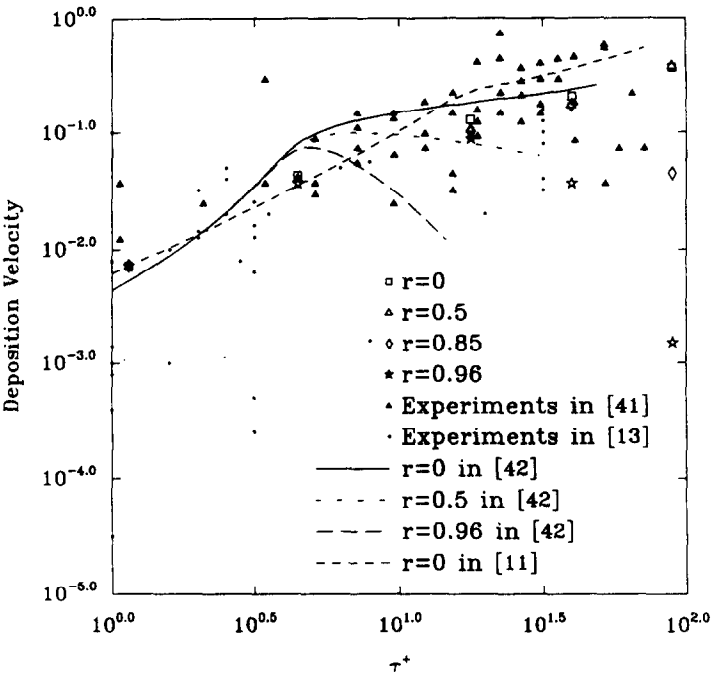

Fig. 16. Particle deposition velocity vs nondimensional particle relaxation time including rebound effect for a horizontal channel.

CONCLUSION

In this work, a digital simulation procedure for studying deposition velocity of aerosol particles in turbulent channel flow is developed. An empirical mean velocity profile and the experimental data for r.m.s. turbulent intensities are used. The instantaneous turbulence fluctuation field is simulated by a continuous Gaussian random field model. The particle equation of motion, which includes the fluid drag, the Brownian force, and the Saffman lift force, is solved numerically and ensembles of trajectories for particles of different sizes are generated and statistically analyzed. The cases of horizontal and vertical channels for which the gravitational effect becomes important or negligible are studied. The effect of particle–surface interaction is also considered. Based on the presented results, the following conclusions may be drawn:

(1) The simulation results are in good agreement with the experimental data and are in qualitative agreement with the empirical equation of Wood and digital simulation of McLaughlin.
(2) Gravitational effect significantly increases the deposition velocity for particles larger than 2 μm.
(3) In the vertical channel, the minimum deposition rate occurs for particle diameters in the range of 1.0–5.0 μm. For the horizontal channel, the gravitational effect shifts the position of minimum to the 0.1–0.5 μm size range.
(4) In the time duration of about 400 wall units, almost all deposited particles originate from the region within 30 wall units from the wall.
(5) The simulation results, including particle rebound effects, are in reasonable agreement with the experimental data and theoretical model predictions.
(6) Rebound effects become noticeable for particles larger than 10 μm.
(7) For particles larger than 10 μm, as the coefficient of restitution increases, the deposition velocity decreases.

Acknowledgements—Thanks are given to Raymond G. Bayer, Michael A. Gaynes and Allen Smith of IBM-Endicott and Dr Douglas W. Cooper for their many helpful suggestions and comments. The financial support of IBM-Endicott is also gratefully acknowledged. The latter stages of this work were also supported by the New York State Science and Technology Foundation through the Center for Advanced Material Processing (CAMP) of Clarkson University.

REFERENCES

[1] D. W. COOPER, *Aerosol Sci. Techn.* **5,** 287 (1986).
[2] D. W. COOPER, M. H. PETERS and R. J. MILLER, *Aerosol Sci. Technol.* **11,** 133 (1989).
[3] B. Y. H. LIU and K.-H. AHN, *Aerosol Sci. Technol.* **6,** 215 (1987).
[4] N. A. FUCHS, *The Mechanics of Aerosol.* Pergamon Press, Oxford (1964).
[5] C. N. DAVIES, *Aerosol Science.* Academic Press, London (1966).
[6] S. K. FRIEDLANDER and H. H. JOHNSTONE, *Ind. Engng Chem.* **49,** 1151 (1957).
[7] J. W. CLEAVER and B. YATES, *Chem. Engng Sci.* **30,** 983 (1975).
[8] M. FICHMAN, C. GUTFINGER and D. PNUELI, *J. Aerosol Sci.* **19,** 123 (1988).
[9] L. W. B. BROWNE, *Atmos. Envir.* 801 (1984).
[10] N. B. WOOD, *J. Aerosol. Sci.* **12,** 275 (1981).
[11] N. B. WOOD, *J. Inst. Energy* **76,** 76 (1981).
[12] G. M. HIDY, *Aerosols, An Industrial and Environmental Science.* Academic Press, New York (1984).
[13] P. G. PAPAVERGOS and A. B. HEDLEY, *Chem. Engng Res. Des.* **62,** 275 (1984).
[14] G. AHMADI and V. GOLDSCHMIDT, *J. Appl. Mech. ASME* **2,** 561 (1970).
[15] R. L. PESKIN, *Digital Computer Simulation of Turbulent Diffusion. In Advanced Computer Methods for Partial Differential Equations,* pp. 207–214. International Association for Mathematics and Computers in Simulations, Rutgers Univ., New Brunswick, N.J. (1975).
[16] H. OUNIS and G. AHMADI, *ASCE J. Engng Mech.* **115,** 2107 (1989).
[17] H. OUNIS and G. AHMADI, *J. Fluids Engng* **112,** 114 (1990).
[18] M. R. MAXEY, *J Fluid Mech.* **174,** 441 (1987).
[19] J. B. McLAUGHLIN, *Phys. Fluids A* **1,** 1211 (1989).
[20] H. OUNIS, G. AHMADI and J. B. McLAUGHLIN, *J. Colloid Interface Sci.* **143,** 266 (1991).
[21] H. OUNIS, G. AHMADI and J. B. McLAUGHLIN, *J. Colloid Interface Sci.* **147,** 233 (1991).
[22] M. A. RIZK and S. E. ELGHOBASHI, *Phys. Fluid* **20,** 806 (1985).
[23] S. ABUZEID, A. A. BUSNAINA and G. AHMADI, *J. Aerosol Sci.* **22,** 43 (1991).
[24] A. LI and G. AHMADI, Dispersion and deposition of spherical particles from point sources in a turbulent channel flow. *J. Aerosol Sci. Tech.* **16,** 209 (1992).
[25] R. H. KRAICHNAN, *Phys. Fluid* **11,** 22 (1970).
[26] P. G. SAFFMAN, *J. Fluid Mech.* **22,** 385 (1965).
[27] G. AHMADI, V. W. GOLDSCHMIDT and B. DEAN, *Iranian J. Sci. Technol.* **5,** 147 (1976).
[28] J. LAUFER, Investigation of turbulent flow in a two-dimensional channel. Report 1053, National Advisory Committee for Aeronautics (1953).
[29] H. P. KREPLIN and H. ECKELMANN, *Phys. Fluids* **22,** 1233 (1979).
[30] F. M. WHITE, *Fluid Mechanics.* McGraw-Hill, New York (1986).
[31] J. O. HINZE, *Turbulence.* McGraw-Hill, New York (1975).
[32] J. T. DAVIES, *Turbulence Phenomena.* Academic Press, New York (1972).
[33] E. G. UHLENBECK and S. L. ORNSTEIN, *Phys. Rev.* **36,** 823 (1930).
[34] S. CHANDRASEKHAR, *Rev. Mod. Phys.* **15,** 1 (1943).
[35] D. GUPTA and M. H. PETERS, *J. Colloid Interface Sci.* **104,** 375 (1985).
[36] H. OUNIS and G. AHMADI, *J. Aerosol Sci. Technol.* **13,** 47 (1990).
[37] S. K. FRIEDLANDER, *Smoke, Dust and Haze.* Wiley, New York (1977).
[38] B. DAHNEKE, *J. Colloid Interface Sci.* **37,** 342 (1971).
[39] B. DAHNEKE, *J. Colloid Interface Sci.* **40,** 1 (1972).
[40] R. H. DAVIS, J.-M. SERAYSSOL and E. J. HINCH, *J. Fluid Mech.* **163,** 479 (1986).
[41] W. KVASNAK, Experimental investigation of dust particle deposition in a turbulent channel flow. M.S. thesis, Mech. Aeronautical Engng Dept, Clarkson Univ., Potsdam, New York (1991).
[42] F.-G. FAN and G. AHMADI, A sublayer model for turbulent deposition of spherical particles in a vertical duct. Report No. MAE-231 May, Mech. Engng Dept, Clarkson Univ., Potsdam, New York (1991). Also *J. Aerosol Sci. Technol.* In press.
[43] M. W. REEKS, *J. Aerosol Sci.* **14,** 729 (1983).

(Revision received 27 February 1992; accepted 3 May 1992)